A Novel Study on The Trend Surface of Posterior Malleolar Fractures

Yichao Ma , Rongjiang Li , Liping Bai , Han Tang , Lixian Bai , Zhijian Ma *

Posted Date: 27 September 2024

doi: 10.20944/preprints202409.2192.v1

Keywords: posterior malleolar fractures; trend surface; spatial geometry; internal fixation; ankle stability

Article

A Novel Study on The Trend Surface of Posterior Malleolar Fractures

Yichao Ma [1], Rongjiang Li [2], Liping Bai [3], Han Tang [2], Lixian Bai [4] and Zhijian Ma [2,*]

[1] School of Medicine, Wuhan University of Science and Technology, Wuhan, 430065, Hubei Province, China
[2] Department of Sports Medicine, The First People's Hospital of Kunming, Kunming, 650051 Yunnan Province, China
[3] Department of Gastroenterology, Affiliated Hospital of Yunnan University, Kunming, 650021 Yunnan Province, China
[4] Department of Neonatology, People's Hospital of Yuxi City, Yuxi, 653310 Yunnan Province, China
* Correspondence: davidrochest@139.com

Abstract: Background: Posterior malleolar fractures (PMFs) account for 7-44% of all ankle fractures, and are crucial for ankle stability, associated with poorer functional outcomes and higher rates of traumatic arthritis. Despite the exact mechanism and treatment strategy of this kind of fractures still remain controversial, most orthopaedic surgeons tend to treat PMFs with open reduction internal fixation method. To achieve rigid fixation for the fragment, screws should be inserted across the fracture plane perpendicularly. However, the study on the spatial geometry of the fracture surface of PMFs, especially the trend surface, has not been reported before. **Objective:** This study aimed to construct the trend surface of PMFs and establish an algorithm to better understand the spatial geometry of the fracture surface, which could guide treatment strategies. **Methods:** A retrospective analysis of CT images of PMFs from January 2021 to January 2024 was conducted. Cases were grouped according to the Bartoníček classification system. The skeletal ankle models were reconstructed, which were then transformed into CAD models. Fracture surfaces were segmented, and point clouds were output to record coordinate values. The K-Dimensional Tree data structure was built for the efficient indexcality of the Depth-First-Search algorithm to find the matched points in the clouds. The average point was computed for matched points, and subsequently, the fracture trend surface and heat map were generated. **Results:** Twenty-four cases were included. The posterior malleolar fracture trend surface was composed of two surfaces, each approximated as a plane and intersect an angle about 130.5°. The posterolateral surface extended slightly curvingly from the posterior two-fifths of the fibular notch to the posteromedial one-third of the distal tibia, formed an angle of 10.1° with the tibia axis and 10.1° with the coronal plan of the lower leg. The posteromedial surface extended from the posteromedial one-third of the distal tibia towards the intercollicular groove, formed an angle of 5.2° with the tibia axis and 39.4° with the coronal plan of the lower leg. The heat map revealed that the high-frequency fracture regions presented at 16.0mm away from the posterior malleolar distal edge and 11.2mm medial to the posterior margin of the fibular notch. **Conclusion:** The study provides a novel perspective on PMFs by describing the spatial geometric morphology of the fracture surface. This can be useful for the treatment strategies. 1. The fracture lines on the bone surface help us generate a stereoscopic model of the fracture surface in our brain, but this model may not be the same as the true fracture surface. 2. In A-P fluoroscopic view, 16.0mm away from the posterior malleolar distal edge and 11.2mm medial to the posterior margin of the fibular notch were the high frequency regions where the fracture surfaces passed through. 3. To firmly hold the posterolateral PMF, 3 key screws should be parallelly inserted into the distal tibia through the fragment, oriented medially 10.4°, cephalad 10°. The insertion points of the screws, in back view, are individually identified at 8.3mm, 16.9mm, 8.3mm superior to the inferior margin of the posterior malleolus, and 6.0mm,10.5mm, 15.1mm posterior to the posterior margin of the fibular notch. The depth of the screws should be no more than 40mm to avoid irritating the anterior tendons, vessels and nerves.

 doi:10.20944/preprints202409.2192.v

Keywords: posterior malleolar fractures; trend surface; spatial geometry; internal fixation; ankle stability

Background

Ankle fracture happens frequently in lower extremity, accounting for about 6.1% of all fractures. Among this kink of fracture, the posterior malleolus is suffered in 7-44% of them. It is well known that posterior malleolus is crucial to obtain ankle stability. Patients with posterior malleolar fractures (PMFs) appears wors functional outcomes and higher accident of traumatic arthritis, comparing those without PMFs. Good reduction an strong fixation are two key points to treat intra-articular fractures. It was thought that avulsion posterior malleolar fragment (PMF) was induced by rotational force, and blocky PMF, sometimes was called posterior Pilon fracture, was caused by strike. However, up to now, the exact mechanism of how PMFs happens still remains controversial. To explain the mechanism and gain better outcomes of PMFs, different classifications were reported, such as Lauge-Hanson classification [1], Haraguchi classification [2], Bartoníček classification [3], etc. All these classifications can be devided into tow groups. The first group is based on X-ray plain film, like Lauge-Hanson classification; the second group is according to CT scan, such as Bartoníček classification. To assess the role of PMFs in maintaining the ankle stability, Su [4], Quan [5], Yu [6], etc. drew the fracture line map to describe the morphology of PMFs. Regrettably, these fracture maps merely stay on the distribution of fracture line on the bone surface, but do not describe the 3D spatial shape of the fracture surface. However, the trajectory of fracture line is not equal to the spatial shape of fracture surface. It is well known that by distributing screws rationally and applying vertical compression, more mechanically effective fixation across the fracture surface can be achieved. So, the screw distribution and insertion direction may be not reasonable based on fracture line map. In order to gain more positive fixation of fracture, it is necessary to obtain the 3D fracture surface. The true fracture map should be the fracture surface map, not just the fracture line map. To achieve this, we studied the PMFs surface, constructed the trend surface, and established the corresponding algorithm.

Materials and Methods

Subjects

Retrospective screening of the CT images for the cases with PMFs was carried out from January 2021 to January 2024. All cases were grouped according to Bartoníček classification system. Inclusion criteria were as follows: 1. type 3 of Bartoníček classification; 2. aged 18 years or older; 3. simple fractures; 4. 1mm CT slice thickness. Cases were excluded if: 1. more than 3 fragments of distal tibia; 2. old fractures; 3. osteoporosis, tumors, tuberculosis, or other destructive diseases around the ankle were noticed.

Generating the Trend Surface of PMFs

CT images were input into Materialise Mimics Medical software (Version 21.0, Materialise NV, Leuven, Belgium) to generate skeletal ankle models in STL format. Then, the STL models were imported into Magic Studio 2013 software (version 2012, North Carolina, USA), and the STL models were transformed into CAD model in STP format based on NURBS surface. After that, a randomly chosen medium-sized ankle model was uploaded in Rhino software (Rhino 6, Robert McNeel & Associates, Seattle, Washington, USA) as the benchmark for model size and coordination adjustment. All models were uploaded in Rhino sequentially and modified size and spatial position according to the benchmark model through ‘zoom, translate, rotate’ order by a senior orthopedic surgeon. Thereafter, fracture surfaces were segmented, their point clouds were output to record the coordinate value (Figure 1). The K-Dimensional Tree data structure was built for the efficient indexcality of the Depth-First-Search to find the matched points in the clouds [7,8]. The euclidean distance between

 doi:10.20944/preprints202409.2192.v

two points on the plane X-O-Y was computed, 0.5mm was set as the threshold to group the points as the 'matched (x,y)' (Figure 2). The number of the points was noted as the frequency of this group. The average value of z in the matched (x,y) point group was calculated, and the average value of (x,y) was also computed. A point could only be included in a matched (x,y) point group once. If there was a point that had no matched points, its (x,y,z) was recorded as this group's ($\bar{x}$, $\bar{y}$, $\bar{z}$). Hence, the matrix of average point cloud [($\bar{x}$, $\bar{y}$, $\bar{z}$)] was built. Subsequently, the matrix [($\bar{x}$, $\bar{y}$, $\bar{z}$)] was imported into Rhino, and the fracture trend surface was reconstructed (Figure 1). Meanwhile, different color was assigned to the corrspoing point accodring to its frequency, so that the heat map of PMFs was built.

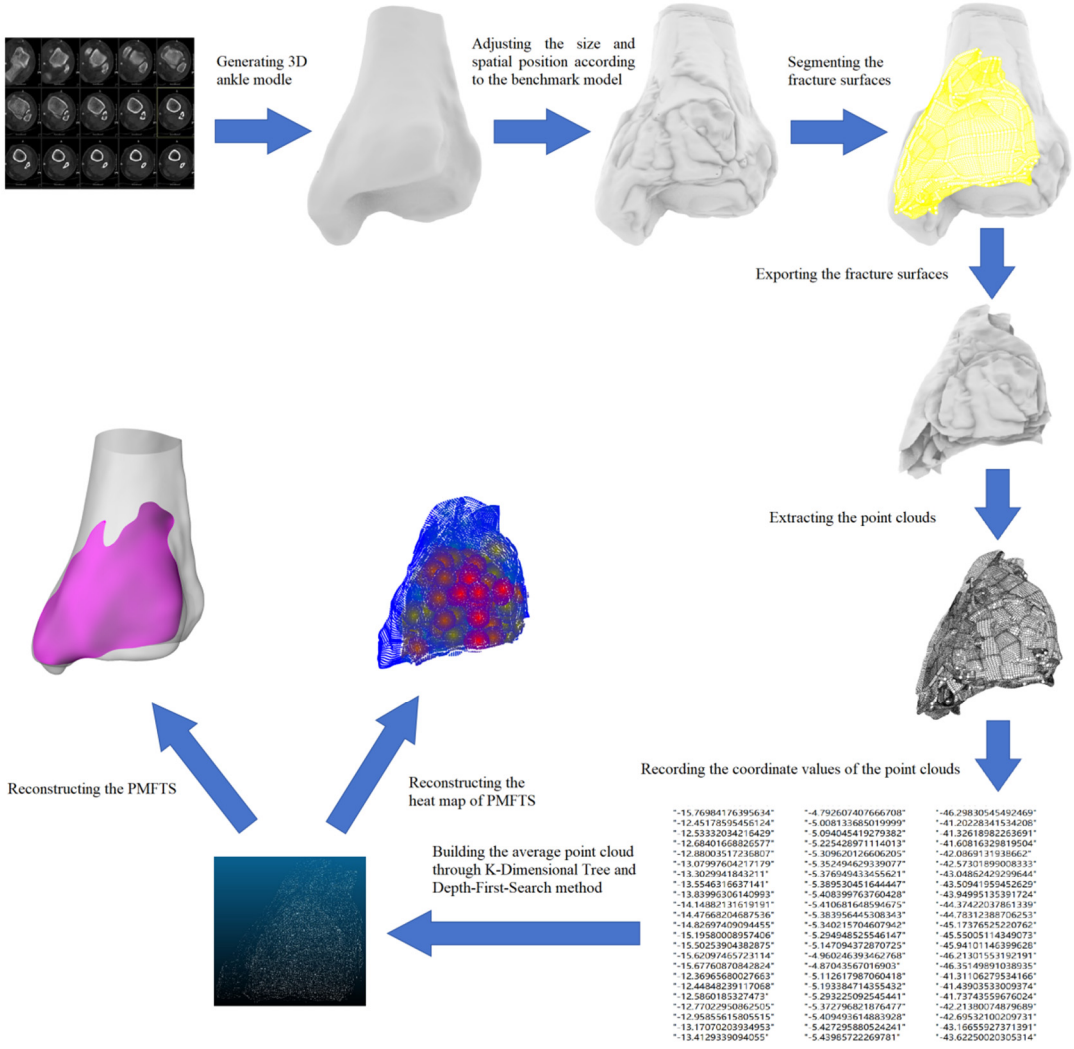

Figure 1. Reconstructing the trend surface of PMFs.

 doi:10.20944/preprints202409.2192.v

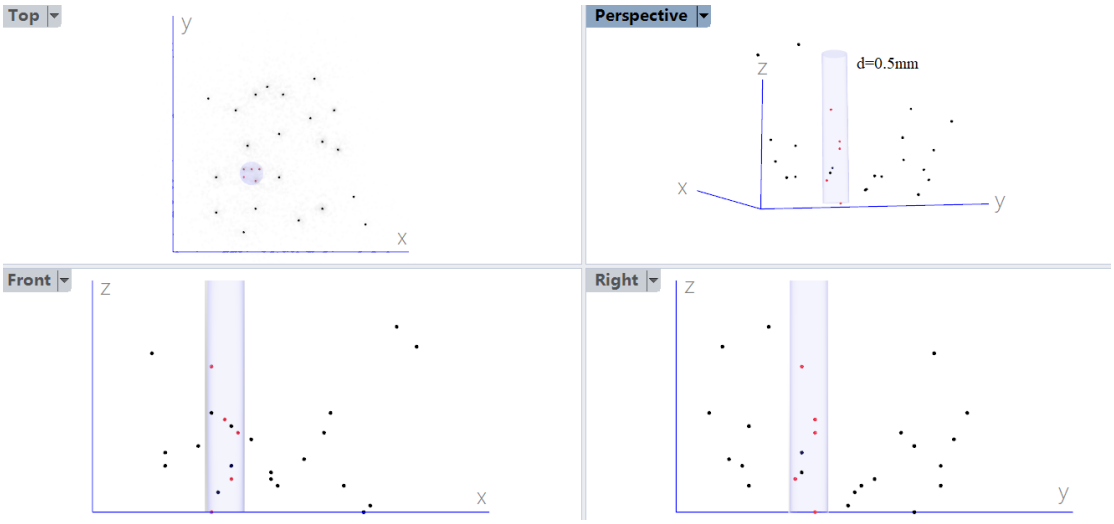

Figure 2. If the euclidean distance between two points on the plane X-O-Y is smaller than 0.5mm (blue column), the points are included in one 'matched (x,y)' group (red points).

Results

A total of 24 cases were included in the study. By applying the least square method, the average point cloud was derived from those 24 fracture point clouds. Subsequently, the posterior malleolar fracture trend surface was fitted based on the average point cloud (Figure 3). Investigating the individual posterior malleolar fracture surfaces and posterior malleolar fracture trend surface (PMFTS), the following findings are revealed. 1. The PMFTS was mainly composed of two surfaces. Although both fracture trend surfaces were unsmooth and slightly curved, each trend surface could still be approximated as a plane. The posterolateral one extended slightly curvingly from the posterior two-fifths of the fibular notch to the posteromedial one-third of the distal tibia, split the posterolateral aspect of the distal tibia. This surface formed an angle of 10.1° with the tibia axis, 23.6° with the line connecting the tips of the medial and lateral malleolus, and 10.1°with the coronal plan of the lower leg (Figure 4). The posteromedial one extended from the posteromedial one-third of the distal tibia towards the intercollicular groove of the medial malleolus, splitting the posteromedial aspect of the distal tibia. This surface formed an angle of 5.2° with the tibia axis, 25.9° with the line connecting the tips of the medial and lateral malleolus, and 39.4° with the coronal plan of the lower leg (Figure 5). The intersection angle between these two surface was 130.5°. Examining the fracture line of the fracture trend surface, in the lateral view, the fracture line ran posteriorly and superiorly from the posterior two-fifths of the fibular notch, forming an angle of about 9.7° with the tibia axis; in the medial view, the fracture line traveled posteriorly and superiorly from the intercollicular groove, forming an angle of about 21.3° with the tibia axis; in the bottom view, the fracture line could be regarded as being composed of two lines, the posterolateral line and the posteromedial line. The former started at the posterior two-fifths of the fibular notch, the latter originated from the intercollicular groove, and these two fracture lines met at medial one-third of distal posterior tibia, intersecting at an angle of approximately 130.6°(Figure 3). Studying the heat map of PMFTS, it was demonstrated that, in the posterior-anterior perspective view, 16.0mm away from the posterior malleolar distal edge and 11.2mm medial to the posterior margin of the fibular notch were the high frequency regions where the fracture surfaces passed through (Figure 6.).

 doi:10.20944/preprints202409.2192.v

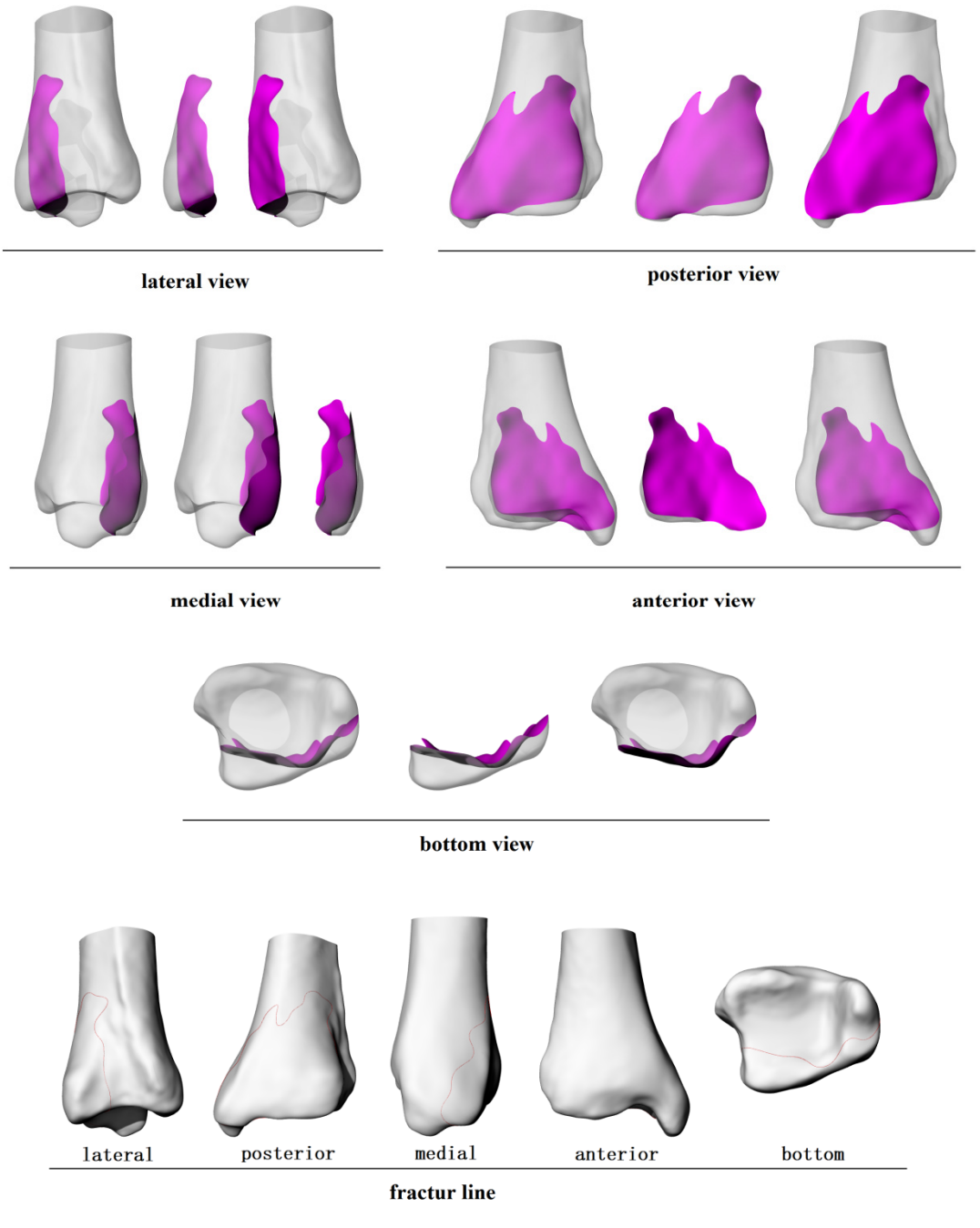

Figure 3. The fracture trend surface of posterior malleolar fracture.

 doi:10.20944/preprints202409.2192.v

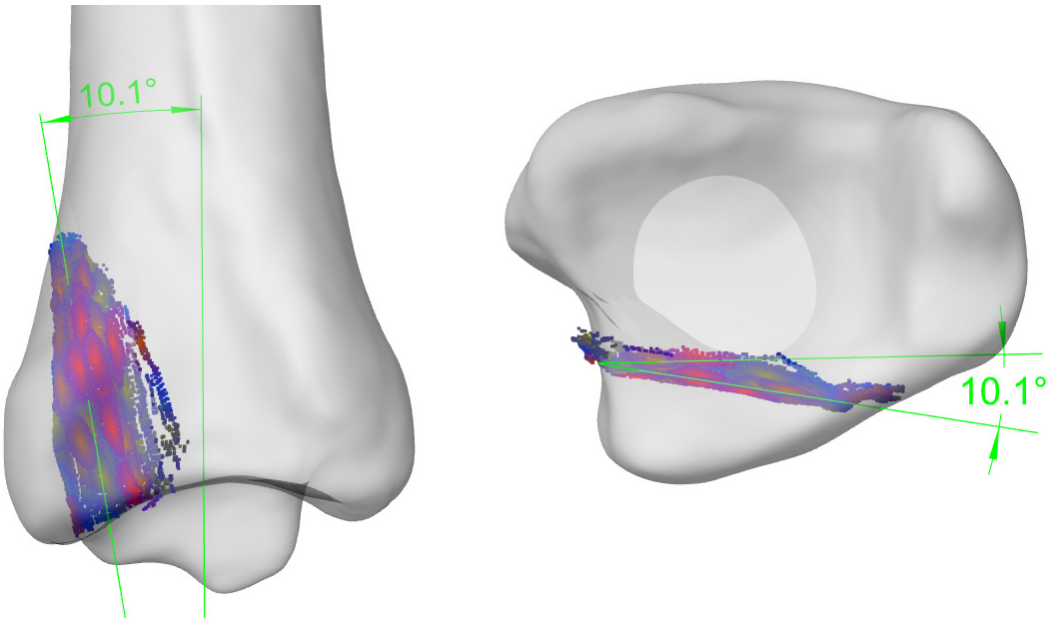

Figure 4. The posterolateral fracture trend surface extended slightly curvingly from the posterior two-fifths of the fibular notch to the posteromedial one-third of the distal tibia, split the posterolateral aspect of the distal tibia. This surface formed an angle of 10.1° with the tibia axis, 23.6° with the line connecting the tips of the medial and lateral malleolus, and 10.1°with the coronal plan of the lower leg.

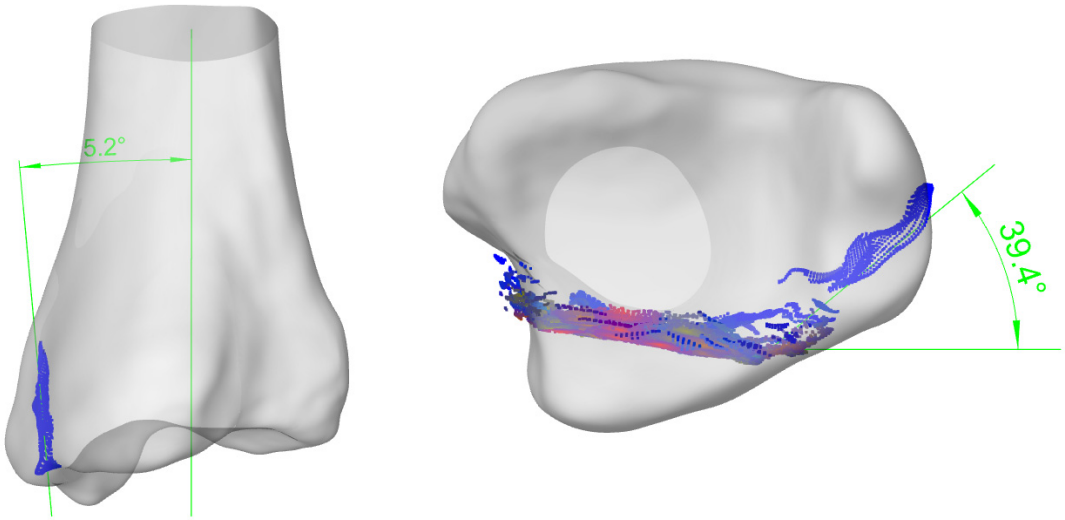

Figure 5. The posteromedial fracture trend surface extended from the posteromedial one-third of the distal tibia towards the intercollicular groove of the medial malleolus, splitting the posteromedial aspect of the distal tibia. This surface forms an angle of 5.2° with the tibia axis, 25.9° with the line connecting the tips of the medial and lateral malleolus, and 39.4° with the coronal plan of the lower leg.

 doi:10.20944/preprints202409.2192.v

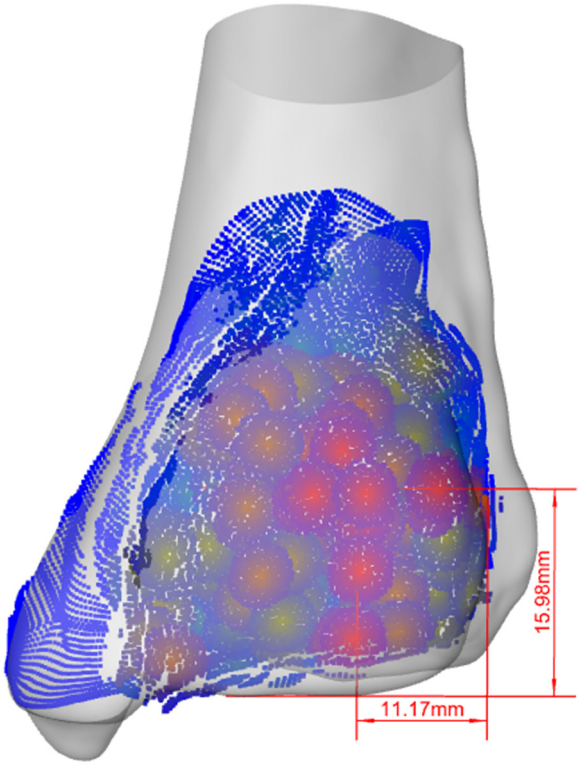

Figure 6. Areas, 16.0mm away from the posterior malleolar distal edge and 11.2mm medial to the posterior margin of the fibular notch, were the high frequency regions where the fracture surfaces passed through.

Discussion

The Epidemiology of PMFs

Ankle fractures is a common kind of injury suffering the lower extremity.In China, 2014, the morbidity of ankle fracture was 3.7/10,000 person-years; the incidence rate among males was 50.5%, while among females, it was 49.5%; the incidence rate is highest among males over 80 years old and females aged 65 to 79 [9]. In USA, 2012-2016, the incidence rate of ankle fracture was 4.22/10,000 person-years; 44% of ankle fractures occurred in men, whereas 56% occurred in women; the highest incidence in men occurred in 10 to 19 years age group, but women were more commonly affected in all other age groups [10]. In both countries, falls was the most popular injury mechanism. Posterior malleolus is usually affected in ankle fractures, occurs in up to 46% of Weber B or C ankle fracture and is rarely isolated [11]. The age group of 50–59 years old stands at the peak of accidence, the number of cases according to different fracture types is as following: trimalleolar fracture-supination external rotation (71.0%) > bimalleolar fracture (12.7%) > trimalleolar fracture-pronation extorsion (9.1%) > posterior malleolus + tibial shaft fracture (4.0%) > simple posterior malleolus fracture (3.2%) [12]. Additionally, posterior malleolar fracture is noticed associated with spiral tibial diaphyseal or shaft fracture. In Hou's study of 288 tibial shaft fracture cases, 28 cases (9.7%) was found with PMFs, but only nine of them were observed preoperatively in plain X-ray films [13]. Posterior malleolus plays a crucial role in ankle stability. Compared with those without PMFs, patients with PMFs tend to have a poorer prognosis and a higher incidence of traumatic ankle arthritis [14]. Not only because the posterior malleolus is the essential component of weight bearing articular surface of ankle mortise, but also it provides the indispensable support for syndesmosis. In recent years, an ascending amount of literature has recommended fixation method for PMFs.

 doi:10.20944/preprints202409.2192.v

The Classification of PMFs

To category the ankle fractures and optimize the outcomes of treatment, many classification systems were reported. Among them, the Lauge-Hanson classification is more popular because that it is closely related with the injury mechanism and guide the treatment strategy. However, there are still approximately 5% of the fractures cannot be classified according to the Lauge-Hansen classification [15]. With the usage of CT scan, classification systems based on this image technique were reported, especially focusing on PMFs. Haraguchi categorize the PMFs into 3 types: type I, oblique posterolateral wedge-shaped fragment involving the posterolateral corner of the tibial plafond; type II, transverse fracture line extending from the fibular notch to the medial malleolus; type III, a small, shell-like fragment at the posterior lip of the tibial plafond [16]. Bartoníček divided PMFs into 5 groups: type 1, extraincisural fragment; type 2, posterolateral fragment; type 3, posteromedial, two-part fragments; type 4, large, posterolateral triangular fragment; type 5, irregular osteoporotic fracture [3]. Mason grouped PMFs into 4 types: type 1: extraarticular/ incisura posterior malleolar avulsion fracture; type 2A: the primary posterolateral triangle fragment of distal tibia extends into the incisura; type 2B: subsequent to type 2A, a secondary fragment on the posteromedial aspect of the distal tibia is produced; type 3: coronal plane fracture line involves the whole posterior plafond [17]. These three classification systems are commonly used when describe the PMFs, each has its own strength and weakness. Haraguchi's classification system is favored for its clear descriptions based on CT images, helps guide treatment decisions. However, accurate classification will be difficult when the fracture fragments are small or atypical. Bartoníček's classification system provides more details, considers the position and size of the fragments as well as their role in the ankle stability. It has shown high reliability in the literature and is well correlated with clinical outcomes.Mason's classification system is based on the illustration of the pathomechanics of PMFs, and shows a good interobserver agreement [18]. Bartoníček's classification is considered the most promising due to its inclusion of a treatment algorithm and consistent predictive outcomes. However, all these classification systems have limitations in describing the complexity of posterior malleolar fractures, and none has fully established its dominance in the literature.

The Morphology of PMFs

To disclose the regularities of the morphology of PMFs aiding in the determination of the reduction and internal fixation strategy, fracture map or heat map of posterior malleolar fracture lines were utilized. It is discovered that, the angle between the fracture line and tibia axis in distal tibial sagittal plane was from 3.3° to 63.9° [19]; this angle was negatively correlated with the percentage of fragment area/distal tibial transverse area [20]; compared to the SER4 (Lauge-Hansen supination external rotation stage 4) group, PER4 (pronation external rotation stage 4) group presented larger PMF, but with more extensive and unorganized distribution fracture lines [4]. Quan et al. divided PMFs into large-fragment, small-fragment, small-shell groups and drew the fracture map. They found that in the small-fragment group, the fracture lines cut the posterior third of posterior malleolus margin; while in the big-fragment group, the fracture lines originated from the middle of the fibular notch and ended at the groove of the tibialis posterior and flexor digitorum longus, separated the whole posterolateral distal tibia [5]. In the present study, it was revealed that the posterolateral fracture trend line originated from the posterior two-fifths of the fibular notch and ended at medial one-third of distal posterior tibia, the angle between posterolateral fracture trend surface and tibia axis was 10.1°. These results ate consistent with the prior fracture map researches. However the preceding investigations did not reveal the details of fracture surface. To our knowledge, this study is the first report describing the spatial geometric morphology of the fracture surface of PMFs and modelling the trend surface.

The Treatment of PMFs

It is generally accepted that PMFs involving more than 25% articular surface [21], with displacement more than 1 mm step-off or 2mm gap [22], need surgical treatment. General strategies of

 doi:10.20944/preprints202409.2192.v

internal fixation for PMFs involve the anterior-posterior (AP) indirect reduction + percutaneous screw fixation method and the posterior approach direct reduction + plate or screw fixation method. A retrospective study on trimalleolar fracture fixation methods in a trauma center over 9 years, involving 86 cases, compared the AP percutaneous screw group with the posterior open reduction internal fixation group. The results showed the better functional and radiological outcomes with the posterior-anterior (PA) method [23]. Taking the advantages of detail and accuracy, FEA is more and more used in biomedical test. There are several study comparing the efficiency of different strategies for PMFs internal fixation through FEA. Most of them support that increasing fracture size requires more stable fixation construct, posterior plate afford superior stability and lower PMF displacement [24,25]. Cadaveric biomechanical studies also support this idea. A study assessed the stability of 15 frozen specimen PMFs with 2 AP screws, 2 PA screws, and a posterior T-shaped plate. The study recommended the use of a posterior plate for the fixation of PMFs, since it presented better stability, while AP and PA lag screws exhibited higher stress and fracture step-off, thereby indicating a higher probability of cut-through and fixation loss [26]. However, the treatment strategies of PMFs is controversial. A meta analysis reported that the A-P screw ranked the highest for AOFAS score and the lowest for occurrences of infection and peroneal nerve injury; on the other hand, the P-A screw was superior in VAS score; nevertheless, the posterior plate presented the lowest level of bone arthritis, non-union, the postoperative articular step-off more than 2 mm, and the loss of ankle dorsiflexion more than 5° [27]. A 10-year follow up study showed that despite worse radiographical osteoarthritis was correlated with PMFs step-off more than 1 mm and dislocation/subluxation, the PMF with average size 16.2 ± 7.39% still presented largely satisfactory clinical outcomes. Additionally, pain and functional scores were not depend on PMF size, fracture step-off, dislocation, and syndesmotic injury [28]. A investigation on 8 biomechanical and 25 clinical studies with more than 950 cases advised that the size of PMF is not the only major factor indicating operation, when considering surgery option, the fracture displacement, the stability and the congruency of the joint are also the critical factors affecting the outcomes [29,30]. In a systematic review, complications and functional results on comparison between PA screw and plate fixation for PMFs, it was revealed that no clinical nor radiological significant differences between groups [31]. Interestingly, a retrospective investigation with a follow-up period of 12.5 to 39.4 years, involving 423 cases of open reduction internal fixation for posterior malleolar fragments, demonstrated that patient-reported outcome measures were barely related to pathophysiology but mostly reflected impairment and depression symptoms [32]. In recent years, the impact of PMFs fixation on the syndesmotic stability has been mentioned. A cadaveric study was conducted to evaluate the effectiveness of different methods to restored native tibiofibular and ankle joint kinematics after PMFs. The results showed that, with external rotation, posterior malleolar screws resulted in higher syndesmotic stability comparing with transsyndesmotic suture button, posterior malleolar screws with AITFL augmentation using suture tape brought out best stability of the fibula and ankle joint [33]. Reviewing previous literature, because of wide variability in fragment characteristics and mode of testing made, it is difficult to compare studies and draw conclusions on the need for surgery and method of fixation, strong conclusions on the effects of fracture and fixation on joint contact pressure and stability could not be made [34]. Even so, since the most of PMFs is a kind of intra-articular fracture, based on the basic theory of Association for the Study of Internal Fixation, anatomic reduction and rigid fixation, if there is significant displacement of PMFs, instability or incongruent of ankle joint, PA reduction and internal fixation should be take into account. According to the principle of vector algorithm: when the magnitude of the force is limited, the more perpendicular the force is to the fracture surface, the greater the normal force is applied on it, subsequently, the higher the static friction is generated (Figure 7). Thereby, the screws inserted into the distal tibia to fix the posterolateral malleolar fragment should orient medially 10.4°, cephalad 10° (Figure 8); meanwhile, to fix the posteromedial malleolar fragment, the screws should orient medially 39.4°, cephalad 5.2° (Figure 5).

 doi:10.20944/preprints202409.2192.v

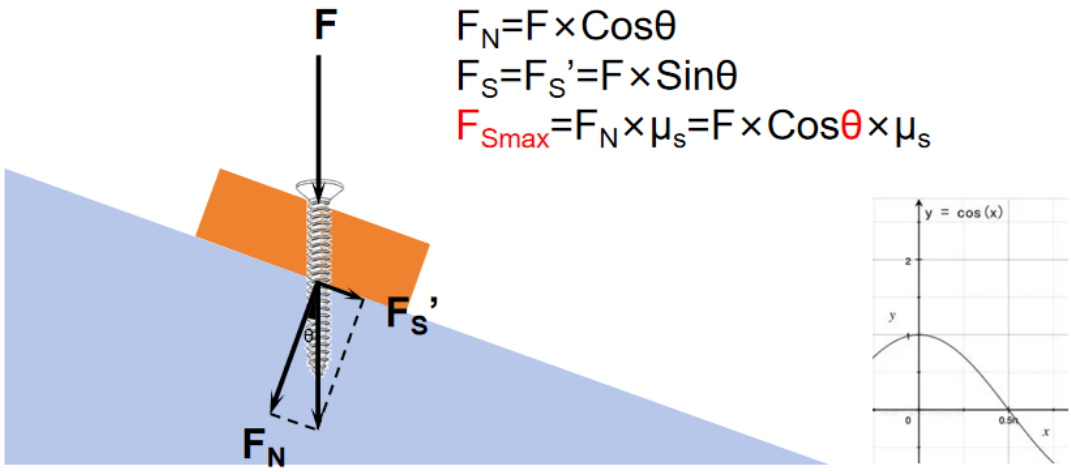

Figure 7. When the magnitude of the force is constant, the smaller the θ is, the greater the maximum static friction becomes.

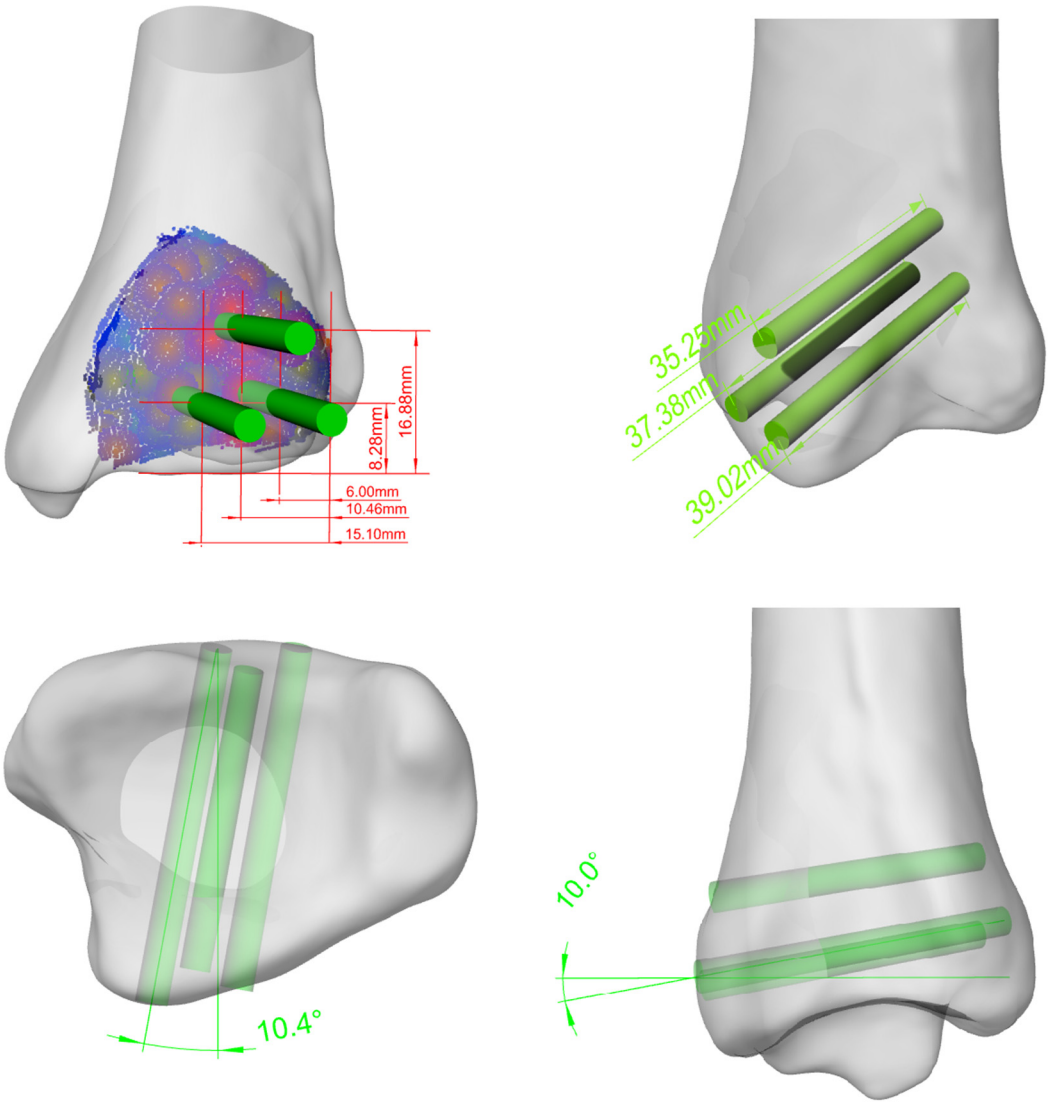

Figure 8. The insertion point, orientation, and the depth of the screws.

 doi:10.20944/preprints202409.2192.v

Limitation and Strength

There are only 24 cases included in the study, more cases need being studied to improve the accuracy of the PMFTS. Nevertheless, the philosophy of this research offers a fresh perspective on understanding the PMFs, and its methods and algorithms will facilitate studies on fractures in other parts of the body, providing a theoretical foundation for exploring fracture mechanisms and improving internal fixation strategies.

Conclusions

1. The fracture lines on the bone surface give us the first impression of the fracture shape. However, these lines are actually the intersection lines of the fracture surface with the bone surface. They help us generate a stereoscopic model of the fracture surface in our brain, but this model may not be the same as the true fracture surface (Figure 3).
2. In A-P fluoroscopic view, 16.0mm away from the posterior malleolar distal edge and 11.2mm medial to the posterior margin of the fibular notch were the high frequency regions where the fracture surfaces passed through (Figure 6).
3. To firmly hold the posterolateral PMF at the reduction place, 3 key screws should be parallelly inserted into the distal tibia through the fragment, oriented medially 10.4°, cephalad 10°. The insertion points of the screws, in back view, are individually identified at 8.3mm, 16.9mm, 8.3mm superior to the inferior margin of the posterior malleolus, and 6.0mm,10.5mm, 15.1mm posterior to the posterior margin of the fibular notch. The depth of the screws should be no more than 40mm to avoid irritating the anterior tendons, vessels and nerves(Figure 8).

Abbreviations

PMFs = Posterior malleolar fractures
PMFTS = Posterior malleolar fracture trend surface
SER = supination external rotation
PER = pronation external rotation
AP = anterior-posterior
PA = posterior-anterior

References

1. Lauge-Hansen N. Fractures of the ankle. II. Combined experimental-surgical and experimental-roentgenologic investigations. Arch Surg. 1950;60(5):957-85.
2. Haraguchi N, Haruyama H, Toga H, Kato F. Pathoanatomy of Posterior Malleolar Fractures of the Ankle. Journal of Bone & Joint Surgery American Volume. 2006;88(5):1085-92.
3. Bartonicek J, StefanKostlivy, KarelVanecek, VaclavKlika, DanielTresl, Ivo. Anatomy and classification of the posterior tibial fragment in ankle fractures. Archives of orthopaedic and trauma surgery. 2015;135(4).
4. Su QH, Liu J, Zhang Y, Tan J, Yan MJ, Zhu K, et al. Three-dimensional computed tomography mapping of posterior malleolar fractures. World journal of clinical cases. 2020;8(1):29-37.
5. Quan Y, Lu H, Xu H, Liu Y, Xie W, Zhang B, et al. The Distribution of Posterior Malleolus Fracture Lines. Foot & ankle international. 2021;42(7):959-66.
6. Yu T, Zhang Y, Zhou H, Yang Y. Distribution of posterior malleolus fracture lines in ankle fracture of supination-external rotation. Revue de chirurgie orthopedique et traumatologique. 2021(6):107.
7. Guo Z, Liu H, Shi H, Li F, Guo X, Cheng B. KD-Tree-Based Euclidean Clustering for Tomographic SAR Point Cloud Extraction and Segmentation. IEEE Geoscience and Remote Sensing Letters. 2023;20:1-5.
8. Yen SH, Shih CY, Chang HW, Li TK, editors. Nearest neighbor searching in high dimensions using multiple KD-trees. International conference on signal processing, computational geometry and artificial visionISCGAV '10; 2011.
9. Song L. Epidemiological study of ankle fractures and risk factors of surgical site infection for adult ankle fractures [Doctor]: Hebei Medical University; 2019.
10. Scheer RC, Newman JM, Zhou JJ, Oommen AJ, Uribe JA. Ankle Fracture Epidemiology in the United States: Patient-Related Trends and Mechanisms of Injury. The Journal of Foot and Ankle Surgery. 2020;59(3):479-83.
11. Bartoníček J, Rammelt S, Tuček M, Naňka O. Posterior malleolar fractures of the ankle. European journal of trauma and emergency surgery: official publication of the European Trauma Society. 2015;41(6):587-600.

 doi:10.20944/preprints202409.2192.v

12. Li Y, Luo R, Li B, Xia J, Zhou H, Huang H, et al. Analysis of the epidemiological characteristics of posterior malleolus fracture in adults. Journal of orthopaedic surgery and research. 2023;18(1):507.
13. Hou Z, Zhang Q, Zhang Y, Li S, Pan J, Wu H. A occult and regular combination injury: the posterior malleolar fracture associated with spiral tibial shaft fracture. The Journal of trauma. 2009;66(5):1385-90.
14. Stringfellow TD, Walters ST, Nash W, Ahluwalia R, Thomas P. Management of posterior malleolus fractures: A multicentre cohort study in the United Kingdom. Foot and Ankle Surgery. 2020;27(6).
15. Van Wessem KJP, Leenen LPH. A rare type of ankle fracture: Syndesmotic rupture combined with a high fibular fracture without medial injury. Injury-international Journal of the Care of the Injured. 2016:766-75.
16. Haraguchi N, Armiger RS. Mechanism of posterior malleolar fracture of the ankle: A cadaveric study. OTA International. 2020;3.
17. Mason LW, Marlow WJ, Widnall J, Molloy AP. Pathoanatomy and Associated Injuries of Posterior Malleolus Fracture of the Ankle. Foot & ankle international. 2017;38(11):1229.
18. Terstegen J, Weel H, Frosch KH, Rolvien T, Schlickewei C, Mueller E. Classifications of posterior malleolar fractures: a systematic literature review. Archives of Orthopaedic and Trauma Surgery. 2022:1-40.
19. Yao L, Zhang W, Yang G, Zhu Y, Zhai Q, Luo C. Morphologic characteristics of the posterior malleolus fragment: a 3-D computer tomography based study. Archives of Orthopaedic & Trauma Surgery. 2014;134(3):389-94.
20. Zhang L, Yang Y, Peng X, Xiong J, Sun X, Xia Z, et al. The Influence of Sagittal Angle of Posterior Malleolus Fracture on Ankle Joint Stability: A Retrospective Study of 120 Cases. Orthopaedic surgery. 2023;15(7):1799-805.
21. Meijer DTD, J. N.Sierevelt, I. N.Mallee, W. H.van Dijk, C. N.Kerkhoffs, G. M.Stufkens, S. A. Guesstimation of posterior malleolar fractures on lateral plain radiographs. Injury. 2015;46(10).
22. Rammelt S, Bartoníček J. Posterior Malleolar Fractures: A Critical Analysis Review. JBJS reviews. 2020;8(8):e19.00207.
23. Erinç S, Cam N. Does It Matter the Fixation Method of The Posterior Malleolar Fragment in Trimalleolar Fractures? Acta chirurgiae orthopaedicae et traumatologiae Cechoslovaca. 2021;88(3):204-10.
24. Anwar A, Lv D, Zhao Z, Zhang Z, Lu M, Nazir MU, et al. Finite element analysis of the three different posterior malleolus fixation strategies in relation to different fracture sizes. Injury-international Journal of the Care of the Injured. 2017;48(4):825–32.
25. Sun D, Shi G, Du K. Biomechanical study of different fixation methods for posterior malleolus fracture. Computer methods in biomechanics and biomedical engineering. 2024;27(9):1141-9.
26. Anwar A, Hu Z, Adnan A, Gao Y, Li B, Nazir MU, et al. Comprehensive biomechanical analysis of three clinically used fixation constructs for posterior malleolar fractures using cadaveric and finite element analysis. Scientific reports. 2020;10(1):18639.
27. Su YC, Wang YY, Fang CJ, Tu YK, Chang CW, Kuan FC, et al. Insights into optimal surgical fixation for posterior malleolar fractures. Bone & joint open. 2024;5(3):227-35.
28. Chong LSL, Khademi MA, Reddy KM, Anderson GH. Ten year outcomes after non-fixation of the smaller posterior malleolar fragment: A retrospective cohort study. The Foot. 2024;59.
29. Odak S, Ahluwalia R, Unnikrishnan P, Hennessy M, Platt S. Management of Posterior Malleolar Fractures: A Systematic Review. Journal of Foot & Ankle Surgery. 2016;55(1):140-5.
30. Serlis A, Konstantopoulos G, Poulios P, Konstantinou P, Ditsios K, Aftzoglou M. The Management of Posterior Malleolus Fractures in Unstable Ankle Injuries: Where Do We Stand Now? Cureus. 2022;14.
31. Sánchez CA, Correal N, Caro D. PA Screw Versus Plate Fixation for Posterior Malleolar Fracture, Systematic Review and Meta-analysis of Complications and Functional Results. The Journal of foot and ankle surgery: official publication of the American College of Foot and Ankle Surgeons. 2024.
32. Meijer DT, Gevers Deynoot BDJ, Stufkens SA, Sierevelt IN, Goslings JC, Kerkhoffs GMMJ, et al. What Factors Are Associated With Outcomes Scores After Surgical Treatment Of Ankle Fractures With a Posterior Malleolar Fragment? Clinical Orthopaedics and Related Research®. 2019;477(4):863-9.
33. Stake IK, Bryniarski AR, Brady AW, Miles JW, Dornan GJ, Madsen JE, et al. Effect of Posterior Malleolar Fixation on Syndesmotic Stability. The American journal of sports medicine. 2023;51(4):997-1006.
34. Stake IK, Douglass BW, Husebye EE, Clanton TO. Methods for Biomechanical Testing of Posterior Malleolar Fractures in Ankle Fractures: A Scoping Review. Foot & ankle international. 2023;44(4):348-62.